STUDY OF COUPLED BUNCH INSTABILITY CAUSED BY ELECTRON CLOUD

K. Ohmi * and S.S. Win
KEK, 1-1 Oho, Tsukuba, 305-0801, Japan

Abstract

Electron cloud induces a transverse wake force which makes a correlation between bunch by bunch, namely a transverse displacement of a bunch causes a perturbation of electron cloud, which affects the transverse motion of following bunches. The correlation can be regard as a kind of wake force. We study the coupled bunch instability caused by electron cloud in drift space and in weak solenoid field, using semi-analytic method and numerical simulation. The mode spectra and growth rate well reproduces experimental results, for example, change of them with or without a solenoid magnetic field.

INTRODUCTION

Positron or proton beam creates electrons due to synchrotron radiation, its loss and secondary emission of absorption of themselves. In the case of multi-bunch operation with a narrow bunch spacing, electron cloud is build-up in the vacuum chamber by their successive production. The beam passes though the cloud as interacting with it. The motion of bunches is correlated each other by the cloud, if memory of previous bunch is remained in electron cloud. If one bunch oscillates with a betatron amplitude, other bunches are affected by the motion of the bunch via electron cloud, with the result that a coupled bunch instability is caused. We discuss the transverse and longitudinal dipole mode instability in this paper.

The transverse coupled bunch instability caused by electron cloud had been observed in some positron storage rings, KEK-PF [1], APS [2] and BEPC [3]. The instability has been observed in KEKB-LER. Mode spectrum characterizes unstable coupled bunch mode has been measured by a fast beam position monitor. Many solenoid magnets were covered vacuum chambers whole of the ring to avoid the single bunch electron cloud effects [4] which limits the luminosity in KEKB-LER. The solenoid magnets were used for studying the characteristics of the coupled bunch instability [5].

To analyze the coupled bunch instability, a photoelectron cloud model has been used [6]. A wake force induced by electron cloud is obtained in the model. Growth rate of each coupled bunch mode is evaluated by the wake force.

The interaction between bunch train and electron cloud is also simulated by a tracking method. The tracking method gives evolution of transverse amplitude of bunches. The growth rate of each mode is obtained by the Fourier analysis of the amplitude evolution, and is compared with that given by the wake force.

We discuss the instability for several cases in KEKB. Parameter of KEKB is shown in Table 1.

Table 1: Basic parameters of the KEKB LER

variable	symbol	KEKB-LER
circumference	L	3016 m
beam energy	E	3.5 GeV
bunch population	N_b	$3.3 - 5.0 \times 10^{10}$
bunch spacing	$t_{sp} = L_{sp}/c$	2-8 ns
rms beam sizes	σ_x	0.42 mm
	σ_y	0.06 mm
bunch length	σ_z	4 mm
synchrotron tune	ν_s	0.024
betatron tune	$\nu_{x(y)}$	45.51/43.57
damping time	$\tau_{x(y)}/T_0$	4000 turn
chamber radius	R	0.05 m

EQUATION OF MOTION

We focus dipole coupled bunch motion of positron bunch. Structures in a bunch is not cared: that is, a bunch is characterized by a transverse/longitudinal position (dipole moment) as a function of s. Interactions between beam and electrons in a cloud is determined by transverse and longitudinal profiles of the beam. The transverse and longitudinal profiles are assumed Gaussian with the deviation determined by the emittance and the average beta function of the transverse and longitudinal direction. Motion of electrons is determined by the interaction with beam, space charge force of themselves and magnetic field. The equations of motion are expressed as

$$\frac{d^2\boldsymbol{x}_p}{ds^2} + K(s)\boldsymbol{x}_p = \frac{r_e}{\gamma}\sum_{e=1}^{N_e}\boldsymbol{F}(\boldsymbol{x}_p - \boldsymbol{x}_e)\delta_P(s - s_e) \quad (1)$$

$$\frac{d^2\boldsymbol{x}_e}{dt^2} = 2r_e c^2 \sum_{p=1}^{N_b}\boldsymbol{F}(\boldsymbol{x}_e - \boldsymbol{x}_p)\delta_P(t - t_p(s_e)) + \frac{e}{m_e}\frac{d\boldsymbol{x}_e}{dt}\times\boldsymbol{B} - \frac{e}{m_e}\frac{\partial\phi}{\partial\boldsymbol{x}}, \quad (2)$$

where indices p and e of $\boldsymbol{x}$ denote the positron and electron, r_e the classical electron radius, m_e the electron mass, c the speed of light, e the electron charge, σ the transverse

* ohmi@post.kek.jp

beam size, ϕ the normalized photoelectron potential, δ_P, the periodic delta function for the circumference, and F the Coulomb force in two-dimensional space expressed by the Bassetti-Erskine formula. In actual calculation, single kick is too strong to simulate electron motion, $\delta(s-s_e)$ has a width of σ_z, $\boldsymbol{F}$ is sum of several (typically 5-10) kicks (or slices) using the formula. The transverse coordinate of each slice in a bunch is an unique value, since only the dipole moment of the bunch is concerned.

The normalized electric potential, which represents interactions between electrons, is determined by Poisson equation,

$$\triangle_\perp \phi(x) = \sum_{a=1}^{N_e} \delta(x - x_{e,a}). \tag{3}$$

The space charge force is solved by Green function including the circular (cylindrical) boundary condition depending on the shape of vacuum chamber.

The electron cloud build-up is estimated by using Eq. (2) with stand alone. Initial condition of electrons are given by a model for example as is seen in Figure 1 [6]. We consider a longitudinal position of a ring characterized by $s_e(+nL)$. Electrons are created when the positron bunch arrives at s_e, namely $t = t(s_e)$. The photo-emission due to synchrotron radiation is dominant for positron rings. The number of photon hitting the chamber wall is given by

$$n_\gamma(/m \cdot e^+) = \frac{5\pi}{\sqrt{3}} \frac{\alpha\gamma}{L}, \tag{4}$$

for a positron in a meter, where α and γ are 1/137 and the relativistic factor, respectively. The number of photo-electron produced by a positron at the chamber is given by

$$n_{e\gamma}(/m \cdot e^+) = n_\gamma Y_\gamma. \tag{5}$$

The direct photo-emission rate was estimated to be $Y_\gamma \sim 0.1$. Typical production rate is $n_{e\gamma} = 0.015 e^-/(\mathrm{m}{\cdot}e^+)$ for example of KEKB. For proton ring, proton loss is considered as a dominant source. The rate is $n_{ploss} = 10^{-6} \sim 10^{-5} e^-/(\mathrm{m}{\cdot}p)$ for example. Ionization is a common source for positron and proton ring. The electron production is generally very small for vacuum pressure of ordinary accelerator: $n_I \sim 1 \times 10^{-8} e^-/(\mathrm{m}{\cdot}e^+(p))$ at 2×10^{-7} Pa.

Secondary electrons are produced with the probability ($\delta_2(E)$) when an electron is absorbed at the chamber wall. The probability, which is a function of energy of the absorbed electron (E), is given typically as follows [7, 8],

$$\begin{aligned} \delta_2(E) &= \delta_0 \exp(-5E/E_{\max}) \\ &+ \delta_{2,\max} \times \frac{E}{E_{\max}} \frac{1.44}{0.44 + (E/E_{\max})^{1.44}}. \end{aligned} \tag{6}$$

The electrons are built-up at a certain density which is determined by balance of creation and absorption of electrons moving under the forces and the initial condition.

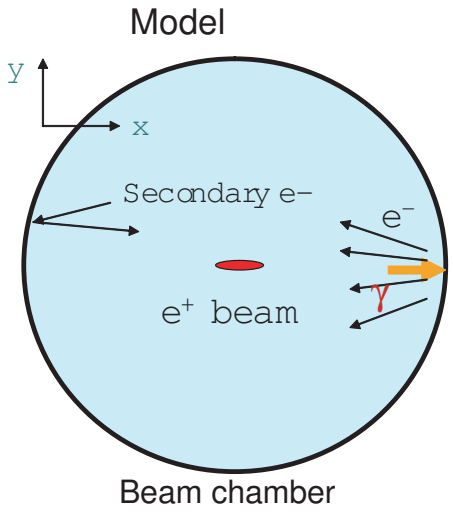

Figure 1: Schematic view of simulation of the electron cloud build-up.

WAKE FIELD AND GROWTH RATE OF THE COUPLED BUNCH INSTABILITY

The coupled bunch effect is simulated by solving the equations, Eq. (1), (2) and 3) with the initial condition self-consistently. It is not very difficult to simulate the evolution of the each bunch amplitude as observing the its instability growth. However this method requires much computer resources and is time consuming. From another point of view, it does not permit us to be imaged a physical picture of the instability. An approximation often makes the physical picture to be transparent. The mechanism, causes instability is similar as the ordinary instability due to vacuum chamber structure. The correlation between bunches is induced by coherent motion of electrons in the cloud or electro-magnetic field in the chamber.

The ordinary instability theory is based on the wake field. The force, which a bunch with z experiences, is expressed by convolution of the wake field (W) and dipole moments of bunches ahead ($z_i < z_j$),

$$F_y(z_i) = \frac{N_p r_e}{\gamma} \sum_{j>i}^{\infty} W(z_i - z_j) y_j(z_j), \tag{7}$$

where the wake field $W(z)$ is a function of the distance between the analyzing bunch (z_i) and the bunches with a dipole moment (z_j). A bunch with a larger i is ahead from smaller. The convolution is based on linearity and superposition of the wake force.

Electrons stay near beam position oscillate with the frequency

$$\omega_e = \sqrt{\frac{2\lambda_p r_e}{\sigma_{x(y)}(\sigma_x + \sigma_y)}} \tag{8}$$

where $\sigma_{x(y)}$ is the horizontal (vertical) beam size. The bunches frequently come but the spacing between bunches

are much longer than bunch length for the positron ring, $\omega_e L_{sp}/c \gg 1$, therefore electrons are not trapped by the beam potential, with the result that most of electrons move in nonlinear region. In this situation, it is difficult to understand whether the wake field has linearity and superposition, though the effect is represented by a kind of wake force.

We are interested in coherent effects for a small perturbation of dipole amplitude of the beam. Though motion of each electron is nonlinear, an averaged force may have linearity and superposition characteristics. For example, an electric force in a cylindrical electron distribution is linear, though it depends on $1/r^2$ for each electron. The wake force is probably far from resonator type. Since the electrons are not trapped and are absorbed at the chamber, the memory of a dipole moment of a bunch is lost soon from the cloud.

Macro-scopic point of view, there may be some characteristic frequency, for example it might be a average frequency $\bar{\omega}$ for average beam line density ($\lambda_p = N_p/L_{sp}$), the cyclotron (Larmor) frequency (ω_c) for finite magnetic field, or others.

$$\bar{\omega}_e = \sqrt{\frac{\bar{\lambda}_p r_e}{\sigma_{x(y)}(\sigma_x + \sigma_y)}}, \qquad \omega_c = \frac{eB}{m_e}, \tag{9}$$

We present an analytical model, in which the cloud is considered as a rigid Gaussian with the chamber size. The characteristic frequency is now expressed by

$$\omega_{G,y}^2 = \frac{2\lambda_b r_e c^2}{(\Sigma_x + \Sigma_y)\Sigma_y}, \tag{10}$$

where Σ_x and Σ_y are horizontal and vertical cloud sizes, respectively, and assumed $\Sigma_{x(y)} \gg \sigma_{x(y)}$.

Analytic method

We discuss the interaction of beam with the rigid Gaussian cloud with the chamber sizes. In this model linearity and superposition characteristics are satisfied automatically. For coupled bunch instability, global feature of electron cloud determined the characteristics. Long range force between beam and electrons is not linear for the distance. We expect in this model that the cloud moves with the frequency (ω_G) in global, though individual electrons move with various frequencies. The approach is not applicable for the single bunch instability. For the single bunch instability, local electron distribution is important, therefore the electron frequency in a bunch (Eq. (8))is characteristic frequency [9].

The frequency for our parameter is $\omega_G = 2\pi \times 10^7$ s^{-1}, and phase advance between bunch spacing (8 ns) is less than 1, $\omega_G L_{sp}/c = 0.13$. Therefore coasting beam approximation can be applied. The equation of motion is expressed by

$$\frac{d^2 y_p(s,z)}{ds^2} + \left(\frac{\omega_{\beta,y}}{c}\right)^2 y_p(s,z)$$
$$= -\left(\frac{\omega_{p,y}}{c}\right)^2 (y_p(s,z) - y_e(s,(s+z)/c)) \tag{11}$$

$$\frac{d^2 y_e(s,t)}{dt^2} = -\omega_{G,y}^2 (y_e(s,t) - y_p(s,ct-s)), \tag{12}$$

where $\omega_{\beta,y}$ denotes the angular betatron frequency free from electron interaction. The two coefficients $\omega_{p,y}$ and $\omega_{e,y}$ characterize the linearized force between beam and cloud, and are given by

$$\omega_{p,y}^2 = \frac{2\lambda_c r_e c^2}{\gamma(\Sigma_x + \Sigma_y)\Sigma_y}, \tag{13}$$

where λ_e and $\bar{\lambda}_p$ are the averaged line densities of cloud and beam.

The two equations are combined by using the wake force

$$\frac{d^2 y_p(s,z)}{ds^2} + \left(\frac{\tilde{\omega}_\beta}{c}\right)^2 y_p(s,z)$$
$$= \frac{\lambda_p r_e}{\gamma} \int_z^\infty W_1(z-z') y_b(s,z'). \tag{14}$$

W_1, which is the wake force for the beam-cloud interaction, is expressed by

$$W_1(z)[\mathrm{m}^{-2}] = cR_S/Q \sin\left(\frac{\omega_e}{c} z\right) \qquad \text{for} \quad z < 0, \tag{15}$$

where

$$cR_S/Q = \frac{\lambda_e}{\bar{\lambda}_p} \frac{2L}{(\Sigma_x + \Sigma_y)\Sigma_y} \frac{\omega_e}{c}. \tag{16}$$

We now discuss the quality factor (Q) of the wake force. Eq. (15) mean that Q is infinite and R_S/Q is constant in the well-known impedance model. Considering the two equations, Eqs.(11) and (12), global motion of electrons excited do not damp anymore, therefore $Q = \infty$. However the frequency of each electron seems to spread very wide range. Electrons move with a frequency given by Eq. (13) only during passage of a bunch, and then they are released from the force. Moreover the beam-electron force during the bunch passage is nonlinear for a large amplitude $\sim 1/r$. It is easy to guess that the quality factor is very small ($Q < 1$) due to the wide frequency spread. We now take $Q = 0.2$, though the reason why we take can not be explained clearly. If we had to say, simulations shown later gave the wake force.

The growth rate is given for a given wake force by

$$\frac{T_0}{\tau(\omega_m)} = \frac{2\pi\lambda_p r_e \beta}{\gamma} \frac{Z(\omega_m)}{Z_0}. \tag{17}$$

where Z is impedance which is Fourier transformation of the wake force, and Z_0 is the vacuum impedance. Figure 2 shows the wake force and the growth rate of each coupled bunch mode given by Eq. (17). The cloud density is determined by build-up simulation as $\lambda_e/\lambda_p = 1$. The growth time is obtained as around 30 turns, that is somewhat slower than that given by semi-analytical and tracking methods as is shown later.

In this model, electron cloud was considered as a very low Q resonator with a coherent frequency. It is not obvious whether this model fit our physical image. However considering the result which is roughly consistent with simulations, the model may includes some kinds of nature of the beam-cloud interaction.

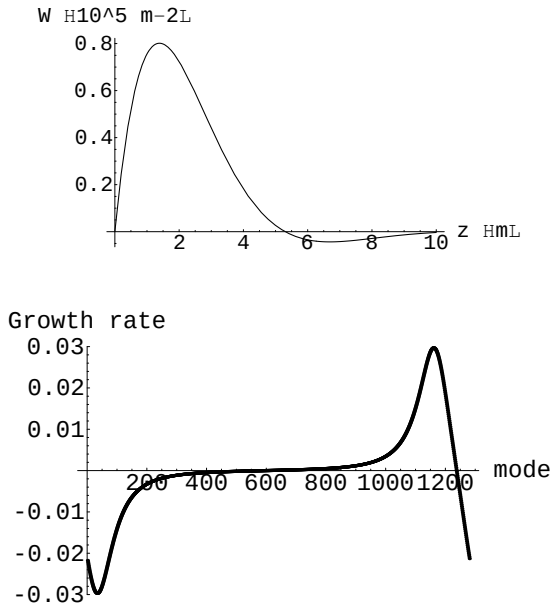

Figure 2: Wake force (a) and growth rate of each coupled bunch mode (b) given by the analytic method at KEKB (2 ns spacing).

Semi-analytical method

We discuss semi-analytic method, in which the wake force is calculated by numerical method and growth rate of each coupled bunch mode is evaluated [6]. This method was used to understand the coupled bunch instability observed at KEK-Photon Factory [1].

We image bunches interact with cloud at a position s. The momentum kick which experiences i-th bunch is expressed by

$$\Delta p_{p,i} = \frac{N_p r_e}{\gamma} \sum_{j>i}^{i+N_w} W(z_i - z_j) y_{p,j}. \qquad (18)$$

This equation is generally used to simulate beam motion for given wake force W. We use this formula to evaluate wake force induced by the electron cloud. Eq. (18) is a linear matrix equation connect Δp_i to y_j. The matrix element, $W(z_i - z_j)$, is determined by response of the momentum kick of a bunch $\Delta p_{p,i}$ for for a displacement of another bunch $y_{p,j}$. The momentum kick ($\Delta p_{p,i}$) is calculated by a simulation, when the displaced bunch with $y_{p,j}$ passes through an electron cloud built-up. Needless to say, the bunch with displacement is ahead of the kicked bunch.

The wake field is evaluated by a computer simulation method as follows,

- Primary electrons are created in every bunch passage through the chamber center with the line density $n_{e\gamma}$. Secondary electrons are created at absorption of an electron with an energy (E_{abs}) by the rate $\delta_2(E_{abs})$.
- The creation process is repeated until the cloud density saturate at a certain value. These two steps is the same is the build-up simulation.
- A bunch with a slight displacement passes through the cloud, and then following bunches without displacement pass through the chamber center.
- The creation process is repeated for the displaced and following bunches.
- The following bunches experience forces from the cloud, because the cloud is perturbed by the passage of the displaced bunch. The wake field is calculated by the forces.

The linearity and superposition are assumed in Eq. (18): that is, the kick $\Delta p_{p,i}$ is sum of when some bunches have displacements, $y_{p,j}$. The simulation have to check whether they are right or not. namely wake force induced by a bunch for several amplitudes, and induced by two or several bunches should be compared.

If linearity and superposition are satisfied for the wake force, the equation of motion gives a dispersion relation,

$$(\Omega_m - \omega_\beta) L/c = \frac{N_p r_e \beta}{2\gamma} \sum_{\ell=1}^{N_w} W(-\ell L_{sp}) \exp\left(2\pi i \ell \frac{m+\nu_\beta}{H}\right). \qquad (19)$$

The imaginary part of $\Omega_m L/c$ is the growth rate per revolution for m-th mode. Bunches oscillate for a mode characterized by m as

$$y_m(z_j) = a \exp\left[-i\Omega t + 2\pi i m j/H\right], \qquad (20)$$

where H is the number of bunch with equal spacing. Real part of Ω is closed to ω_β.

Figure 3 shows the wake force and the corresponding line density of the electron cloud for KEKB, where the bunch repetition is 8 ns. To check the linearity, the wake force (Wy_0) for $y_0 = 1, 2, 5$ mm is evaluated as shown in Picture (a). Here 200-th bunch is displaced and the forces which following bunches experience from electron cloud are plotted. The wake force has a peak at 201-th bunch, which has a linearity for the amplitude of initial displacement (y_0). It oscillates 1 or 2 periods with a much smaller amplitude than the peak. Linearity of the wake force is satisfied up to no more than 210-th bunch. The direction of the wake force is the same as the displacement: that is, it is "defocusing" force for a bunch train. The characteristics is the same as that of ordinary wake force.

The wake force after 210-th bunch is considered to be numerical noise of the simulation. Corresponding cloud

line density is depicted in Picture (b). Beam line density is $5 \times 10^{10}/2.4 \sim 2 \times 10^{10}$ m^{-1}, that is 50% higher than the neutralization level.

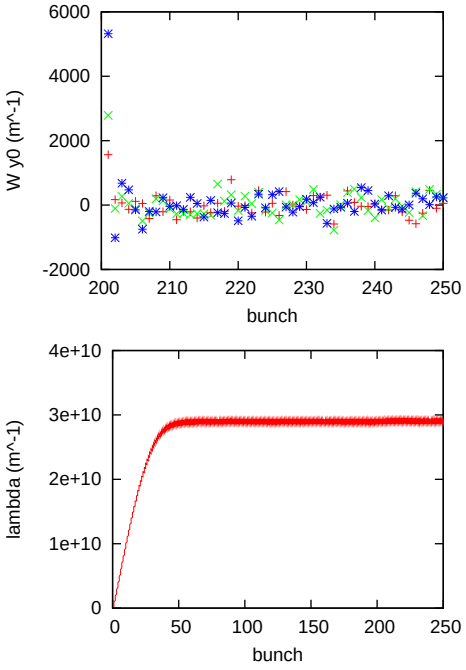

Figure 3: Vertical wake force and cloud density along the bunch train at KEKB. Bunch repetition is 8 ns. Three types of points are given for the displacement, y_0 =1 (red), 2 (green) and 5 mm (blue).

Figure 4 shows the wake force for various bunch spacing keeping the total current. The wake forces for 2, 4 and 8 ns spacing are depicted in picture (a). The wake force does not strongly depend on the spacing as far as is seen in peak strength and range.

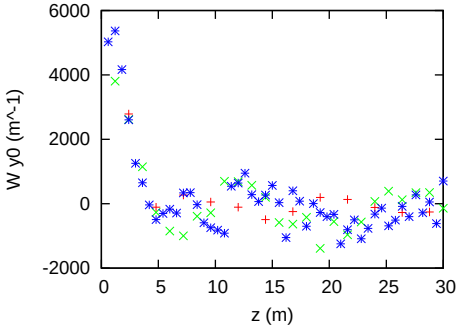

Figure 4: Vertical wake force for 2, 4, and 8 ns spacing as a function of z at KEKB, where $y_0 = 2$ mm.

The wake force little depends on emittance, therefore it can occur also in the horizontal direction. Figure 5 shows the horizontal wake force for $x_0 = 5$ mm. Here the wake force is calculated for 8 ns spacing. Two pictures (a) and (b) are given for two different initial condition of electrons: that is, electrons are produced at illuminated position and low secondary rate, $\delta_2 = 1$ at picture (a), and electrons are produced uniformly along the chamber wall, and with the secondary yield, $\delta_{2,\max} = 1.5$. In the first case, electron distribution is flat along x plane with thickness of 1-2 cm. The direction of the wake force is opposite to the displacement: that is, it is "focusing" for the bunch train. In the second case, electron cloud distributes with cylindrical symmetry, with the result that the wake force is similar as the vertical one.

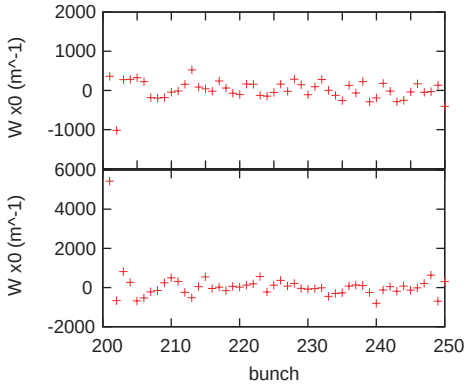

Figure 5: Horizontal wake force for 8 ns spacing at KEKB.

Unstable modes of coupled bunch instability and their growth rate are calculated by Eq. (19). Figure 6 shows the growth rate per revolution for each coupled bunch mode for the vertical instability. The growth rate for 2 and 4 ns spacing is slightly higher than that for 8 ns spacing. For 8 ns spacing, 800-th and 1050-th modes are most unstable. The growth time, which is about 5 turns for every case, is very rapid.

Growth rate of the horizontal mode is shown in Figure 7. Two pictures correspond to the wake forces shown in Figure 5. Picture (a) is given for the condition that electros are produced at illuminated position and low secondary rate, $\delta_2 = 1$, and (b) is for the condition that electrons are produced uniformly along the chamber wall, and with the secondary yield, $\delta_{2,\max} = 1.5$. 150-th mode is unstable in picture (b). The unstable mode less than $H/2 - int(\nu)$ is forward traveling of the coupled bunch oscillation: that is, the betatron phase of backward bunches go forward from those of forward bunches in the coupled bunch oscillation This is characteristics of "focusing" wake in Figure 5(b).

Wake force in a weak solenoid magnetic field

Magnetic field affects the coupled bunch instability through the second term of RHS of Eq. (2). Effects of the magnetic field have been studied since the design stage of KEKB [10, 11, 12, 13]. Electrons experience cyclotron motion, and center of the cyclotron motion drifts along the chamber surface. The cyclotron frequency (ω_c) is $2\pi \times 28$ MHz for $B_z = 10$ G and linearly depends on B_z. The other frequency is obtained by the same manner

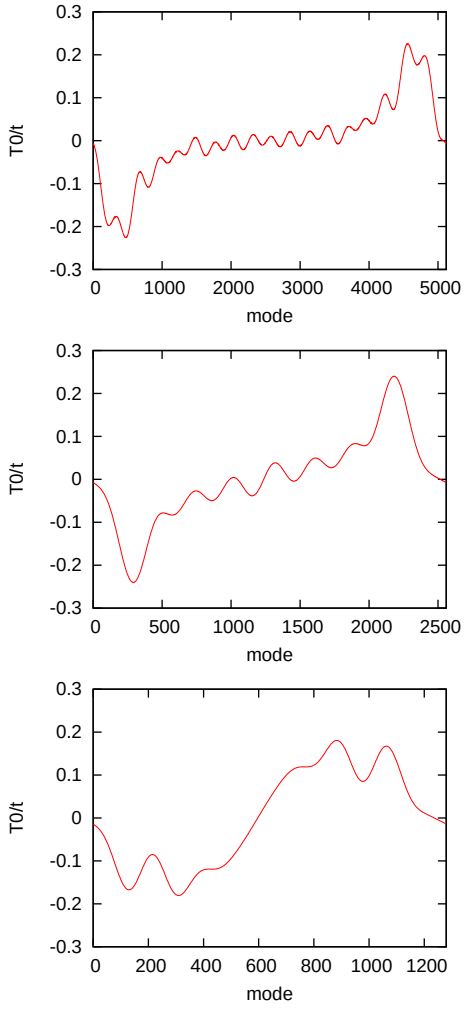

Figure 6: Growth rate of coupled bunch instability. Positive rate means unstable. Pictures (a), (b) and (c) depicts mode spectra for 2, 4 and 8 ns spacing.

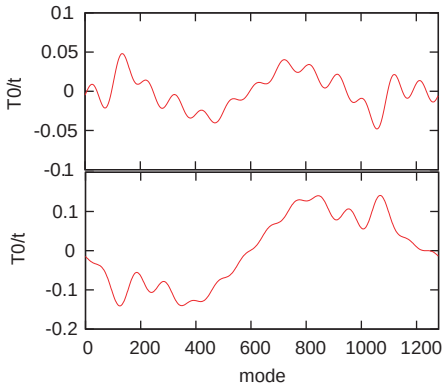

Figure 7: Growth rate of horizontal coupled bunch instability. Pictures (a) and (b) depicts for electron initial conditions: (a) created illuminated point and $\delta_{2,\max} = 1$, and (b) created uniformly and $\delta_{2,\max} = 1.5$.

as the motion in the magnetron. It is expressed by

$$\omega_{\pm} = \frac{\omega_c}{2} \pm \sqrt{\frac{\omega_c^2}{4} - \frac{r_e \lambda_+ c^2}{\bar{r}^2}} \tag{21}$$

where $\bar{r}$ is average orbit radius of electrons. Here the radius is assumed to be larger than Larmor radius. If electrons are created at the chamber wall and are trapped near it by the magnetic field, the radius is closed to the chamber radius R. If some kinds of diffusion occur in the electron motion, the radius may be smaller than the chamber radius. In these two frequency, one (ω_+) is cyclotron frequency slightly shifted by the beam force, and the other (ω_-), which is circulating with a spiral trajectory along the chamber surface [11], is far slower than cyclotron one. Perturbation of the electron motion with the frequencies is induced by a displacement of a bunch, and the coupled bunch instability is subject to the electron motion with the frequencies. Figure 8 shows the frequencies as a function of B_z for $\bar{r} = 5, 4$ and 3 cm. ω_- is faster for electron orbit which approach to the beam position (small $\bar{r}$), while ω_+ is slower.

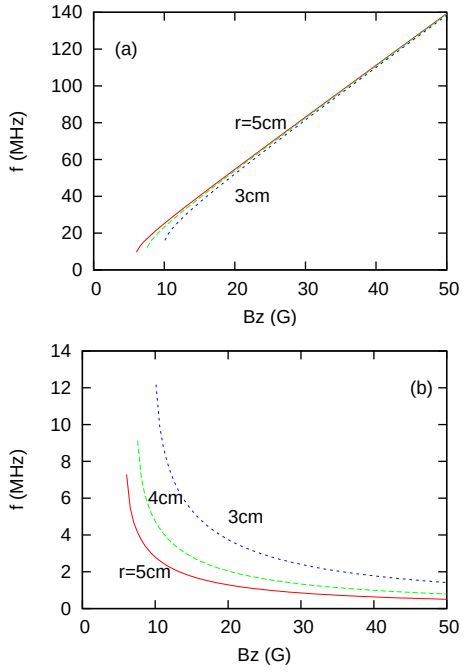

Figure 8: Magnetron frequency as a function of B_z. Pictures (a) and (b) depicts frequency $\omega_+/2\pi$ and $\omega_-/2\pi$, respectively.

Figure 9 shows the wake force for displacement of 600-th bunch of 1, 2 and 5 mm at $B_z = 10$ G. The wake force has a fast frequency component correspond to ω_c or ω_+ and a slow frequency correspond to ω_-. The slow frequency, which is about 4 MHz in Figure 9, is consistent with the frequency given for the orbit radius $\bar{r}$ = 4-5 cm in Figure 8(b). We have to note that the wake force with the slow frequency component has linearity for the displacement, while that for the fast frequency component (ω_c) does not have linearity. This fact means that the instability with the

slow frequency is observed but that with the fast frequency may not be observed. One more important feature of the wake force with ω_- is "focusing" nature at just after the displaced bunch. Such wake force induces unstable mode less than $H/2 - \mathrm{Int}(\nu)$ or more than $H - \mathrm{Int}(\nu)$, which is forward traveling of coupled bunch oscillation, as is discussed in the horizontal instability in Figure 7(a).

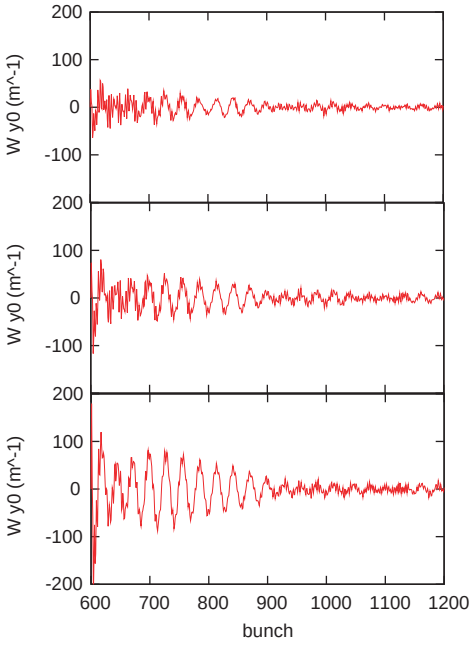

Figure 9: Wake force for various displacement in solenoid field, $B_z = 10$ G. Pictures (a), (b) and (c) depicts the wake force for the 600-th bunch displacements, 1, 2 and 5 mm, respectively.

Figure 10 shows the wake force for $B_z = 20$ and 30 G for the 600-th bunch displacement of 5 mm. Two frequency components are seen in both picture. Again the fast frequency is ω_+ or ω_c. The slow frequencies, which have 60 (2 MHz) and 100 (1.25 MHz) periods for $B_z = 20$ and 30 G, respectively, in unit of bunch, coincides with ω_- in Figure 8. The linearity for the wake force with the slow frequency was statisfied in these field strengths, but that with the fast frequency was unsatisfied,

Figure 11 shows mode spectra of growth modes for $B_z = 10$, 20 and 30 G. To get the spectra, the wake force given by $y_0 = 5$ mm was used. As is expected, forward traveling component of the coupled bunch instability is obtained in the mode spectrum: that is, the mode number is small or more than $H - \mathrm{Int}(\nu_y)$. For $B_z = 10$ G, the slow frequency was 6 MHz in Figure 9, therefore mode with $60 - 43 \sim 20$ appears in Figure 11(a). Note that the revolution frequency is 0.1 MHz. For $B_z = 20$ and 30 G, modes with $20 - 43 + 1280 \sim 1260$ and $12 - 43 + 1280 = 1250$ appears in Figure 11(b) and (c), respectively. The mode spectrum has two frequency component near cyclotron frequency, perhaps one is ω_c and the other is ω_+. However the wake force did not has linearity for the fast frequency component. We have to wait for results of tracking simulation whether the unstable modes with ω_c and ω_+ is observed.

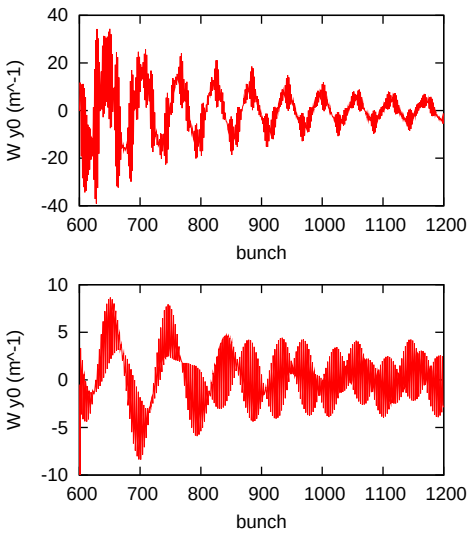

Figure 10: Wake force for $B_z = 20$ (a) and 30 G (b) for the 600-th bunch displacement of 5 mm.

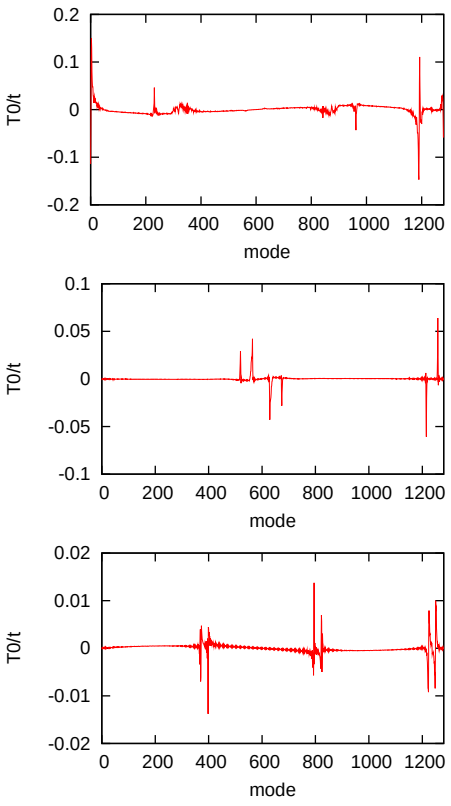

Figure 11: Growth rate of coupled bunch instability for $B_z = 10$, 20 and 30 G.

TRACKING OF THE COUPLED BUNCH INSTABILITY

The three equations, Eq. (1), (2) and (3) can be directly solved numerically [14, 15]. The calculation time is much longer than the wake method. For the wake field calculation, it was sufficient to calculate interactions of several dozens or a few hundreds bunches with electron cloud. In this tracking simulation, bunches in a ring interact with cloud during several thousand or more revolutions depending on the growth time. Since the calculation of the space charge field is consuming, we use an approximation. The Poisson equation is solved only once for zero beam amplitude: that is, the space charge potential, which was calculated by the build-up simulation, is used as a constant field in this tracking simulation. This approximation is reliable and is sufficient for us, when the beam oscillation amplitude is small. Paying the cost of the long calculation time, the nonlinear effect and deviation of superposition for the beam-cloud interaction are included automatically.

The transverse amplitude of each bunch is obtained as a function of time. Fourier transformation of the amplitude of all bunches gives a spectrum of unstable modes. Experiments of coupled bunch instabilities has been done widely using fast position monitors [16]. The bunch centroid amplitude is directly taken by the monitors as a function of time. Mode spectrum given by the Fourier transformation of the experimental data can be compared with that obtained by the simulation.

Figure 12 shows the growth of the coupled bunch instability given by the simulation. Electrons are produced at the illuminated point and parameters for secondary emission is $\delta_{2,\max} = 1.5$ and $\delta_2(0) = 0.5$. $H = 1280$ bunches with an uniform population are put with every 8 ns spacing in the simulation. The evolution of maximum transverse amplitude in bunches is plotted in Picture (a). The amplitude grow exponentially for far smaller value than the chamber size, while is saturated at the order of the chamber size ($\sim$ cm). The growth time is about 10 turn, that is consistent with the estimation using the wake force (5 turns), see Figure 6(c). The snapshot of the transverese position of each bunch after 50 turns is depicted in Picture (b). The oscillation period is unsteadly changed between 5-10 for both plane. The frequency is 20-10 MHz, because of the bunch repetition 125 MHz. Corresponding mode number is 200(100)-45=150(50) for the forward traveling or 1280-45-200(100)=1050(1150) for the backward traveling. The backward traveling is expected from the wake force in previous section.

Figure 13 shows mode spectrum given by Fourier transformation of the amplitude evolution. The amplitudes between 10 through 60 turn, which are in exponential growth regime, are used for the calculation of the mode spectrum. Pictures (a) and (b) depicts the horizontal and vertical spectra, respectively, for electrons emitted at illuminated point. The fast unstable modes distributes around 800-900 in the vertical. In the horizontal spectrum has forward traveling

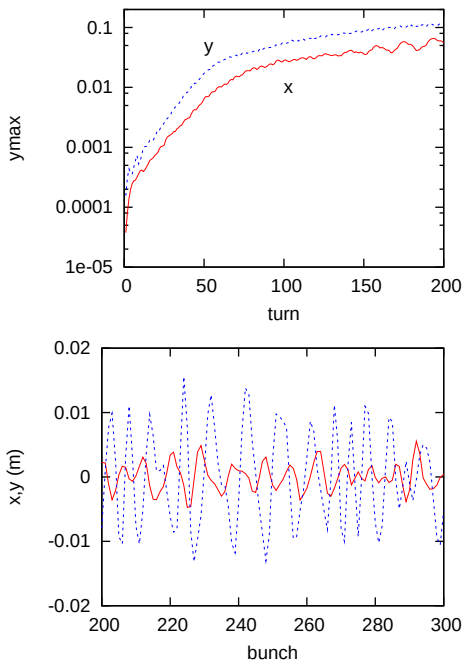

Figure 12: Growth of the hoizontal (x: solid curve) and vetical (y: dotted curve) amplitude (a) and bunch oscillation pattern (b).

mode, 100-200. These pictures are compared with Figure 6(c) and 7(a), respectively. The mode spectra are coincident with those given by the wake force qualitatively. Pictures (c) and (d) depicts for electrons emitted uniformly. Pictures (e)-(h) depicts the same pictures for $\delta_{2,\max} = 1.5$ and reflection is $\delta_2(0) = 0.5$. Horizontal and vertical spectra roughly coincide each other. This fact is due to the cloud distribution is symmetric for high secondary emission rate. The fast unstable modes now distribute around 1000-1100.

Tracking in a weak solenoid magnetic field

As is seen in previous section, the wake force in a weak solenoid magnetic field has two frequency components, ω_- and $\omega_{+(c)}$. A component of the wake force ω_- has linearity for a bunch displacement, but another component $\omega_{+(c)}$ does not have linearity. The tracking simulation gives play to its ability to investigate whether and how the modes with or without linearity is obseved.

Figure 14 shows the growth of the coupled bunch instability for $B_z = 10$ G. Evolution of the maximum transverse amplitude along the bunch train is plotted in Picture (a). The amplitude grows exponentially for the amplitude < 1 cm, and the growth time is about 40 turn.

The growth rate using the wake force in Figure 11 showed 10 turns. Considering the deviation of linearity and superposition of the wake force, the difference may be reasonable. The transverse amplitude of each bunch after 100 turns is depicted in Picture (b). The bunch by bunch os-

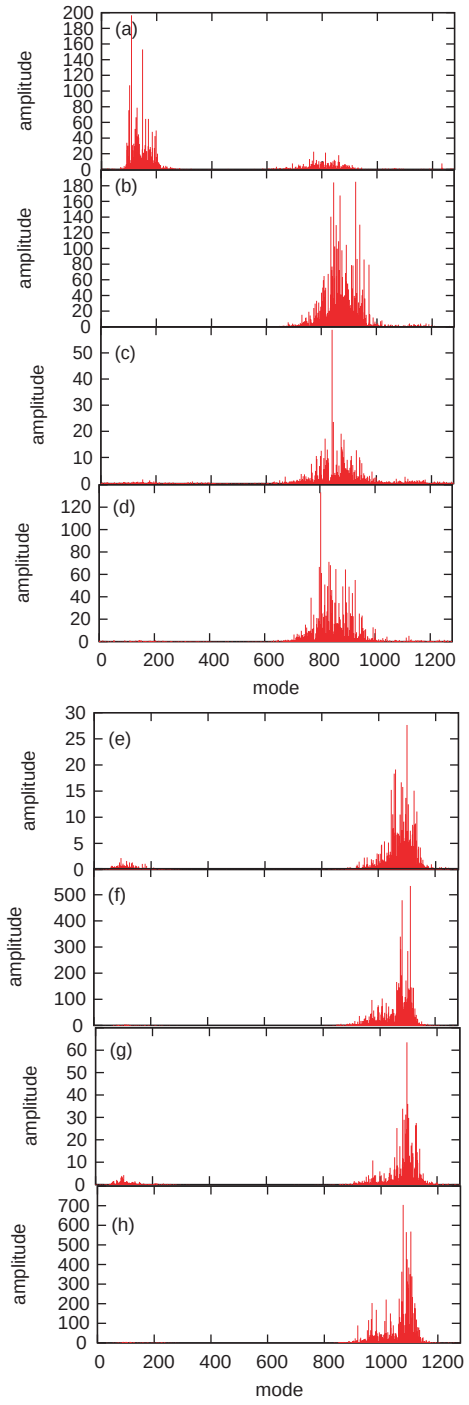

Figure 13: Mode spectrum given by Fourier transformation of the amplitude evolution.

cillation has a slower frequency than that of no magnetic field. The oscillation period is about 20 bunch, namely the frequency is 6 MHz. The slow frequency is consistently with the frequency seen in the wake force (Figure 9)and ω_- (Figure 8). A structure with the cyclotron frequency $\omega_c = 2\pi \times 24$ MHz, that is 5 bunch period, is seen but it is not remarkable.

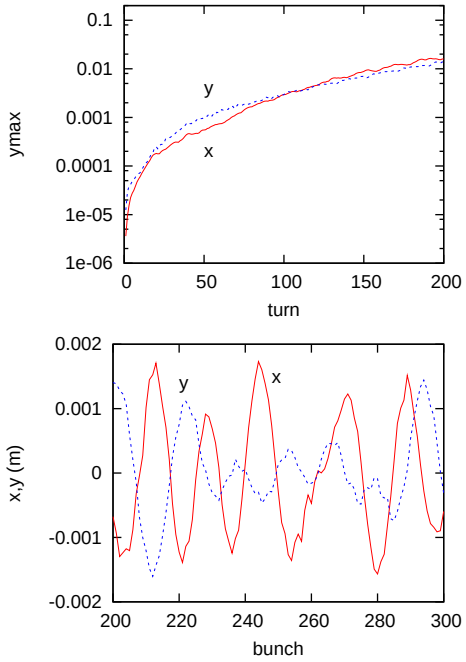

Figure 14: Growth of the amplitude (a) and bunch oscillation pattern (b) for $B_z = 10$ G.

Figure 15 shows the mode spectra obtained by Fourier transformation of the amplitude evolution. As is expected, the mode numbers distribute in 0-50, which means driving frequency of $(43 + m) \times 0.1$ MHz$\sim 4 - 10$ MHz for $B_z = 10$ G in Picture (a). The modes is caused by a focusing wake force with the driving frequency, while a defocusing wake with the frequency causes instability with modes around 1200-1150. The modes 0-50 means the coupled bunch oscillation has a forward traveling with the slow frequency (ω_-).

For higher magnetic field $B_z \geq 20$ G, the modes with very high number is observed. As is predicted in previous section, the modes with 1250-60 are observed in picture (b) and (c). The modes are forward traveling, and qualitatively the same feature as the result of $B_z = 10$ G.

LONGITUDINAL COUPLED BUNCH INSTABILITY

Longitudinal instability was first discussed by G. Rumolo and F. Zimmermann [17] for single bunch effect, then coupled bunch mode of longitudinal instability was proposed by Novokhaski [18].

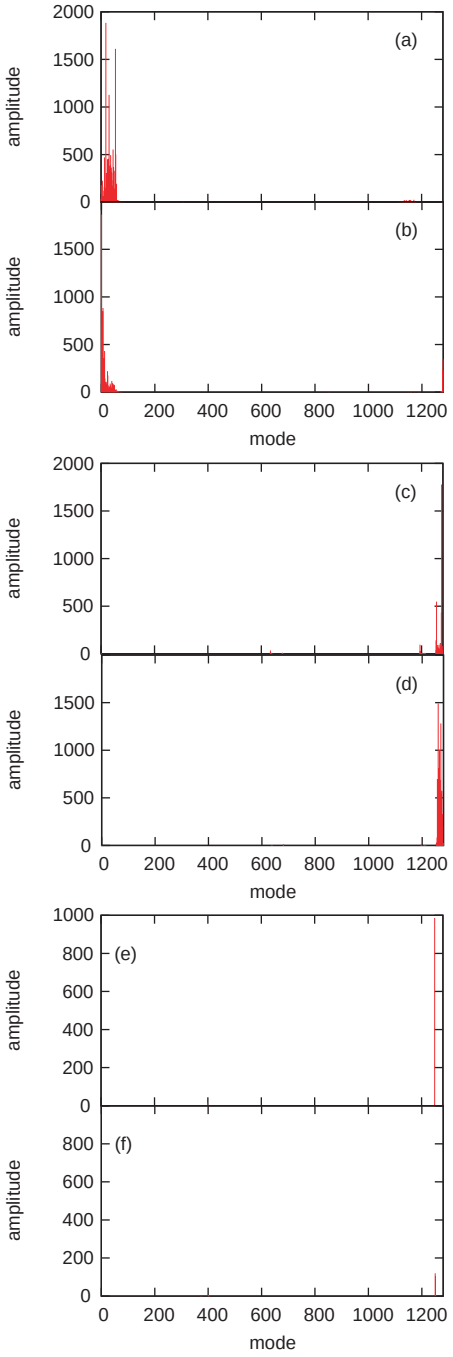

Figure 15: Mode spectra of the coupled bunch instability in week solenoid field. Pictures (a) and (b) are depicted the horizontal and vertical spectra for $B_z = 10$ G, respectively. Pictures (c) and (d) $B_z = 20$ G. Pictures (e) and (f) $B_z = 30$ G.

The longitudinal electric field is calculated for electron cloud with cylindrical symmetry [19].

$$E_z = Z_0 \int_r^R j_r(r', z) dr', \tag{22}$$

where Z_0 is the vacuum impedance and j_r is the radial component of electron current in cloud. The longitudinal wake force is estimated by a similar manner as the case of the transverse wake force.

Figure 16 shows longitudinal electric field as function of time. E_z marked green points is the electric field which bunch experiences. Note that a bunch is represented by 10 slices now.

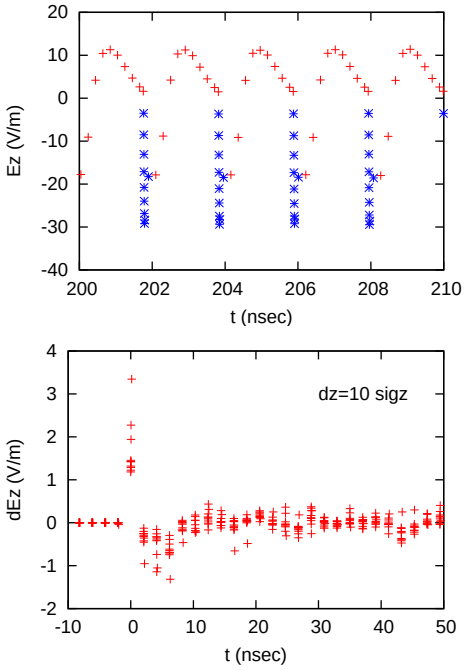

Figure 16: Longitudinal electric field (a) and wake force (b) for KEKB.

The growth rate is obtained by a dispersion relation,

$$\Omega_m - \omega_s = -\frac{N_p r_p \eta c}{2\gamma T_0 \omega_s} \sum_{n=1}^{n_0} W''\left(\frac{n}{H}L\right) \left[1 - \exp\left(2\pi i n \frac{m+\nu_s}{H}\right)\right], \tag{23}$$

where W'' is the same as dE/dz, except coefficients.

The growth rate $\Im(\Omega_m)$ was slower than 0.01 s^{-1} in a preliminary calculation for super KEKB. The longitudinal coupled bunch instability is not serious in present machines.

CONCLUSION

We have studied the coupled bunch instability caused by the electron cloud. The coupled bunch instability is caused

by bunch by bunch correlation due to the electron cloud. The instability was analyzed by analytic, semi-analytic and tracking simulation.

Analytic method showed wake force and mode spectrum using a simple model. Though the choice of Q factor is artificial, growth rate was roughly reasonable.

In the semi-analytical method, the wake force was calculated by simulation. Linearity and superposition are assumed to estimate the mode spectrum of the coupled bunch instability. Wake forces for electrons in drift space and in a weak solenoid field were evaluated. Growth mode of the coupled bunch instability was estimated by the wake force. This method is rather practical, but is not almighty. For example when magnetic field is applied, the wake force is not evidently linear for the amplitude, therefore this method is useless.

The tracking simulation does not use any approximations except that bunch is expressed by its dipole position. The growth rate of each coupled bunch mode was obtained by the Fourier analysis of the dipole amplitudes of bunches given by the tracking simulation. Comparison of the results from the semi-analytic and tracking method made clear the nature of the coupled bunch instability.

The mode spectra for the growth were obtained for electrons in drift space and in a weak solenoid field. The growth rate was very rapid, $\sim$ 10 turn, for drift space. When cloud is cylindrical symmetry in the chamber, instability appears at around 800$\sim$1100-th mode for KEKB 8 ns spacing, $H = 1280$. When the cloud has a flat distribution along the horizontal plane, the horizontal instability appears modes around 100$\sim$200-th.

When a weak solenoid field was applied, the growth rate was reduced: for example it was from 10 to 40 turns for $B_z = 10$ G in the tracking simulation. The wake force has frequency components expressed by Eq. (21). In the tracking simulation, only slow frequency component with ω_- was observed. This feature is reasonable, since the fast frequency component of the wake force did not have linearity for the dipole amplitude. The wake force for the slow frequency was focusing along the bunch train. In the tracking simulation, modes with the forward traveling, whose numbers are near zero or more than 1257=1280-43, were observed as is expected by the focusing wake. It is interesting to explain the focusing wake using an analytic theory.

The forward traveling modes were observed in experiments at KEKB-LER [5]. The measured modes were similar as those obtained for $B_z = 10$ G in the simulation. In the experiments solenoid field with $B_z = 30-40$ G was applied. This fact means that the effective magnetic field was smaller, otherwise electrons stayed nearer the beam than our expectation, $\bar{r} \ll R$ in Eq. (21), for example, electrons were not confined near the chamber due to some kinds of diffusion.

Electron cloud can cause a longitudinal coupled bunch instability. The growth of the instability may not be serious in present positron storage rings.

ACKNOWLEDGMENTS

The authors acknowledge members of KEKB commissioning group, especially H. Fukuma, M. Tobiyama and S. Kurokawa for many discussions on expeiments. They also thank discussions with F. Zimmermann and A. Novokhatski, who motivated the study of the longitudinal instability.

REFERENCES

[1] M. Izawa et al., Phys. Rev. Lett., **74**, 5044 (1995).

[2] K. Harkay et al., Proceedings of ECLOUD02 (2002).

[3] Z.Y. Guo et al., Phys. Rev. ST-AB, **5**, 124403 (2002).

[4] F. Zimmermann, in this proceeding.

[5] S.S. Win et al., Proceedings of ECLOUD02.

[6] K. Ohmi, Phys. Rev. Lett., **75**, 1526 (1995).

[7] M. A. Furman and G. R. Lambertson, Proceedings of the PAC97, 1617 (1997).

[8] V. Baglin, I. Collins, B. Henrist, N. Hilleret and G. Vorlaufer, LHC-Project-Report-472.

[9] K. Ohmi, F. Zimmermann, E. Perevedentsev, Phys. Rev. E **65**, 16502 (2002).

[10] KEKB B-Factory Design Report, KEK 95-7 (1995).

[11] K. Ohmi, Proceedings of APAC98, 435 (1998).

[12] L. Wang et al., Phys. Rev. ST-AB, **5** 124402 (2002).

[13] L. Wang et al., in this proceeding.

[14] K. Ohmi, Phys. Rev. E**55** 7550 (1997).

[15] K. Ohmi, Proceedings of PAC97, 1667 (1997).

[16] M. Tobiyama et al., Phys. Rev. ST-AB, **3** 012801 (2000).

[17] G. Rumolo and F. Zimmermann, Proceedings of ECLOUD02, 147 (2002).

[18] A. Novokhatski, Proceedings of 30-th Advanced ICFA Beam Dynamics Workshop on High Luminosity e^+e^- Colliders, Oct. 13-16, 2003, SLAC.

[19] A. Novokhatski and J. Seeman, SLAC-PUB-10327, Jan. (2004).